Synthesis and Evaluation of Benzohydrazide Derivative as a Corrosion Protector for Magnesium Alloy in 3%Nacl

RAJA KALIYAPERUMAL (krajaphd2012@gmail.com)
ST.JOSEPH UNIVERSITY DIMAPUR https://orcid.org/0000-0002-2887-8398
T.KASILINGAM -
Theivanai Ammal College for Women

Research Article

Keywords: weight-loss technique, Nyquist spectra, Tafel plot, scanning electron microscope, energy dispersive x-ray analysis

Posted Date: March 13th, 2021

DOI: https://doi.org/10.21203/rs.3.rs-288422/v1

SNTHESIS AND EVALUATION OF BENZOHYDRAZIDE DERIVATIVE AS A CORROSION PROTECTOR FOR MAGNESIUM ALLOY IN 3%NaCl

K.Raja[1] and T.Kasilingam[2]

[1]PG and Research Department of Chemistry St.Joseph University Dimapur, Nagaland India.

[2] PG and Research Department of Chemistry, Theivanai Ammal College for Women, Villupuram, Tamilnadu, India.

Corresponding author mail: krajaphd2012@gmail.com

Abstract

Inhibition action of 4-Chloro-N(3,4,5-trimethoxybenzilidene) benzohydrazide on the corrosion of magnesium alloy in alkaline medium was investigated by weight-loss technique, Nyquist spectra, Tafel plot, scanning electron microscope and energy dispersive x-ray analysis. Tafel curves of magnesium alloy showed both anodic and cathodic process suppressed. Nyquist plots, scanning electron microscope and energy dispersive x-ray analysis studies provide the confirmatory evidence for the protection of magnesium alloy by the studied inhibitor.

Keywords: Tafel plot, Nyquist plot, Weight loss technique, SEM and EDX

1. Introduction

Corrosion inhibitors may be categorized in step with chemical structure, approach of motion, and so on. One of the not unusual training is natural corrosion inhibitors that obtained the highest importance because of their ease synthesis at fantastically low fee and high protection ability.[1-5] The method of prevention can be ascribed to the adsorption on the metal floor and impeding the energetic corrosion sites. Formation of protective layer among the competitive answer and steel floor preclude the dissolution of the steel and reduce corrosion damages. organic inhibitors containing heteroatom consisting of N, O, S and P, have tested nearly and theoretically to act as effectively corrosion inhibitors in a wide range of acidic solutions.[6-8] The efficiency of these inhibitors may be attributed to their excessive polarizability and lower electro negativity; so that these atoms and the practical corporations can cowl big steel floor regions and effortlessly electrons transfer to the empty orbitals of atoms. similarly, nitrogen-containing natural inhibitor is good anticorrosion materials for metals in hydrochloric acid, at the same time as compounds having sulfur atoms act as accurate inhibitors in sulfuric acid. [9-15] Compounds conserving nitrogen and sulfur behave as ideal corrosion inhibitors for both media . The motion of any inhibitor for any particular metallic alloys in sever acidic environments relies upon on the nature of the function inhibitor film gathered at the metal surface and the number and nature of adsorption centers contributing within the adsorption manner.[16-23] In preferred, the inhibition

2.Experimental methods

2.1 Synthesis of 4-chloro-N'-(3, 4, 5-trimethoxybenziliden) benzohydrazide

0.17g of 4-Chlorobenzohydrazide and 0.091g 3, 4,5-trimethoxybenzaldehyde were mixed in ethanol and continuously stirred for half an hour and addition of Con. HCl in 2 drops keeping the reaction mixed on a magnetic stirrer. The white solid obtained filtered and recrystallized using ethanol. The purity of the compound was checked with TLC. The melting point was determined from Schiff base compound.

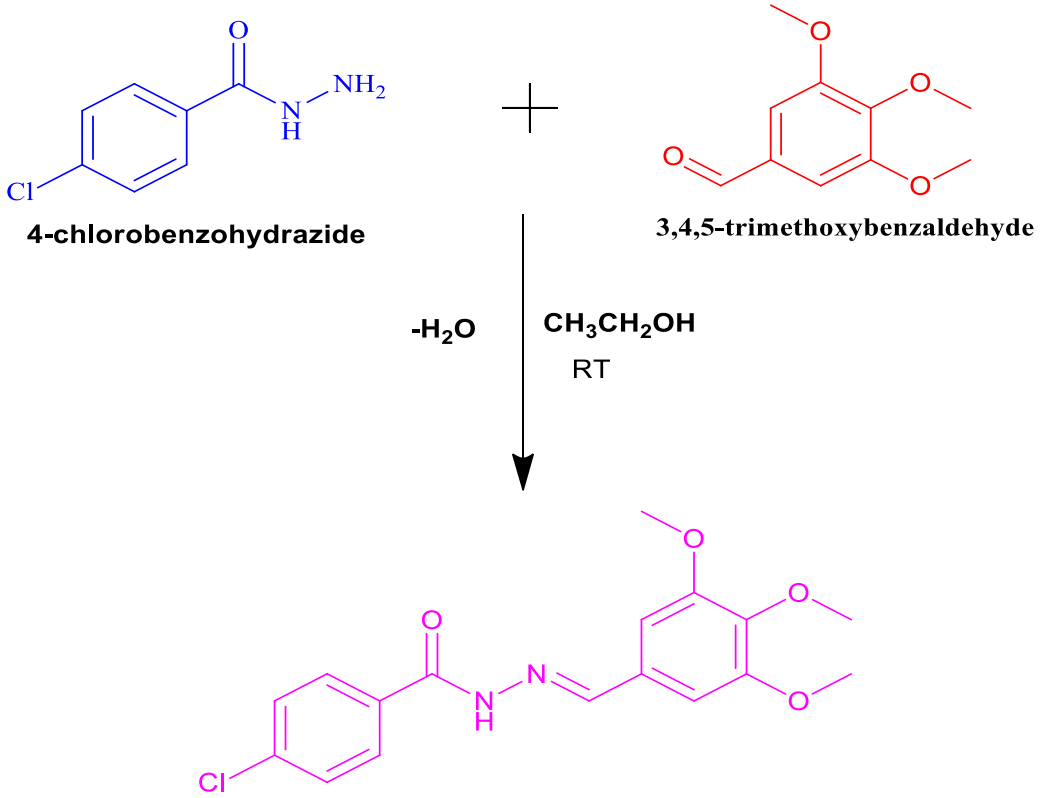

4-chlorobenzohydrazide

3,4,5-trimethoxybenzaldehyde

(*E*)-4-chloro-*N*'-(3,4,5-trimethoxybenzylidene)benzohydrazide

SCHEME

2.2 SPECTRAL ANALYSIS

2.2.1 FT-IR SPECTRUM OF 4CTMBB

IR absorption spectra were recorded in the 4,000–400 cm^{-1} range on a Shimadzu FTIR-8400s using KBr pellets technique. The infrared spectroscopy is one of the most powerful analytical techniques used, which offers the possibility of identification of functional groups present in the compound.

Table :1: FT-IR spectrum of 4CTMBB

S. No	Compound	IR Spectra (cm^{-1})
1	N-H –group	3126
2	Ar –CH group	2943
3	Ali –CH group	2840
4	(C=O) group	1640
5	(C-N)group	1542
6	(C-O)group	1132

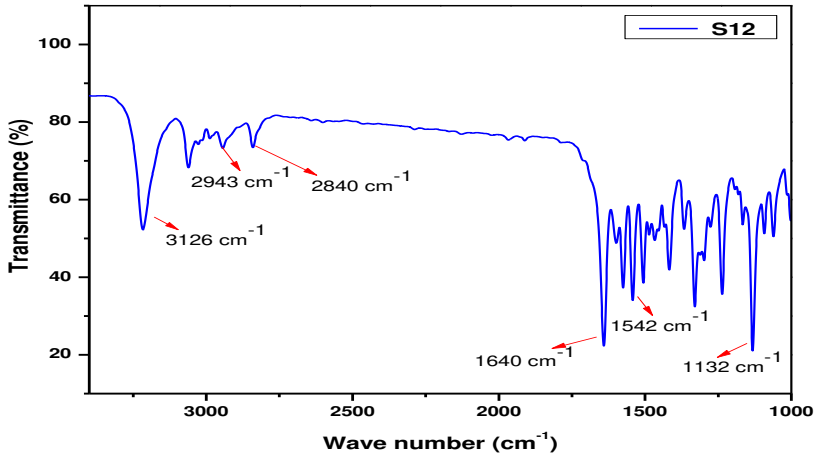

Figure 1 FT-IR spectrum of 4CTMBB

2.2.2 ^{1}HNMR SPECTRUM OF 4CTMBB

^{1}H-NMR and ^{13}C-NMR spectra were recorded on a Bruker-300MHz spectrophotometer. The ^{1}H-NMR and ^{13}C-NMR chemical shifts are reported as parts per million (ppm) downfield from TMS (Me_4Si) used as an internal standard. The spectra were recorded with DMSO/$CDCl_3$ as a solvent. The splitting patterns are designated as follows; s- singlet; d- doublet; m-multiplet.

Table 2: ^{1}H NMR spectrum of 4CTMBB

S. No	Compound	^{1}H NMR ($CHCl_3$) (δ) (ppm)
1	(N-H) Proton	9.3
2	(CH=N) Proton	8.2
3	Ar(C-H)Proton	7.8
4	Ar(C-H)Proton	7.4 – 6.9
5	(OCH_3)Methoxy group	3.8

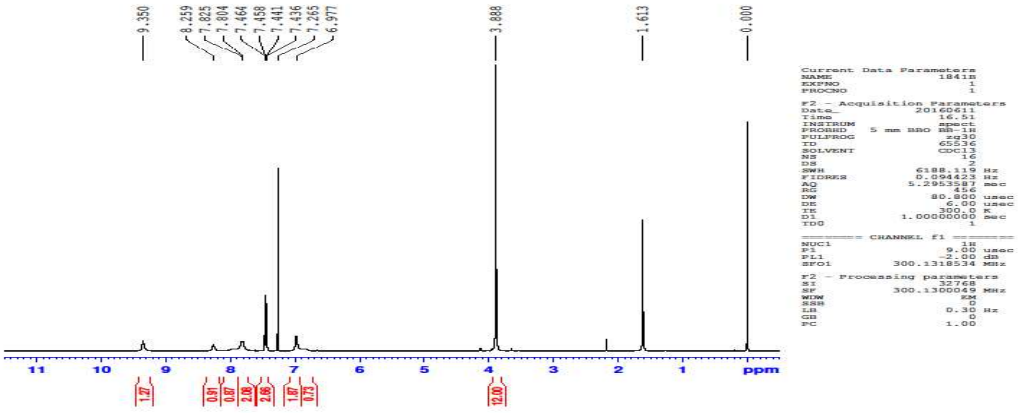

Figure 2: ^{1}H NMR spectrum of 4CTMBB

2.2.3 ^{13}C NMR SPECTRUM OF 4CTMBB

Table 3: ^{13}C NMR spectrum of 4CTMBB

S NO	Compound	^{13}C-NMR ($CHCl_3$)(δ) (ppm)
1	(C=O)Carbonyl group	163
2	(CH=N)Azo group	153
3	Ar(C-H) group	149
4	Carbonyl compound	137-40.03

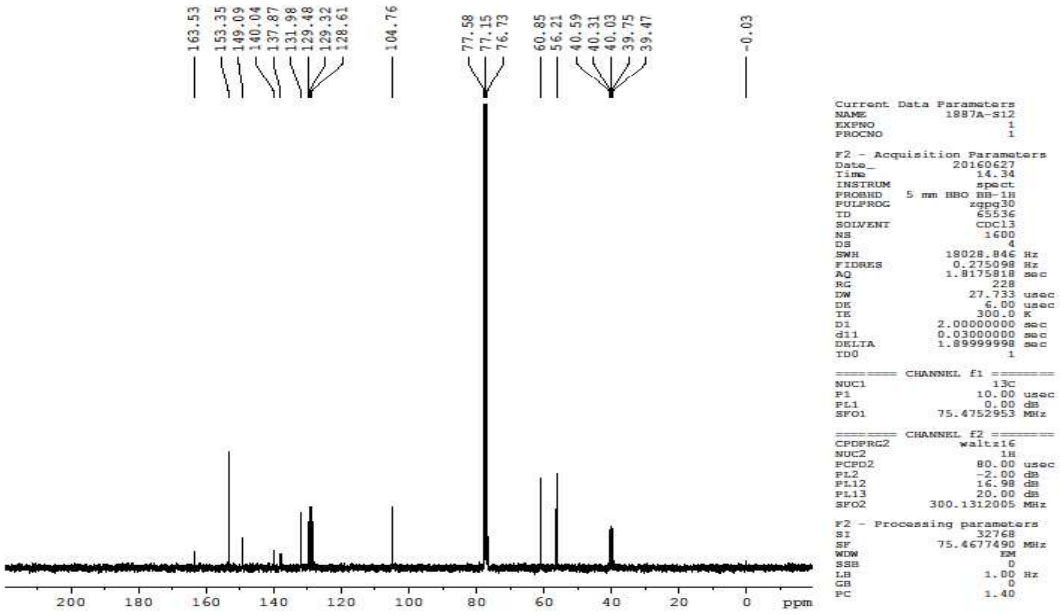

Figure 3: ^{13}C NMR spectrum of 4CTMBB

3. Electrochemical studies

3.1 Mass loss measurement

With recognize to the determination of corrosion charge, the maximum correct and particular approach is probably mass loss measurement . The mass loss elevated with the immersion period which illustrated the development of corrosion. That IE% growth with increasing the protector awareness in 3% NaCl environment. This indicates that the protecting effect of protector is not entirely due to their reactivity with the alkaline medium. The protector conduct of the 4CTMBB towards corrosion of magnesium alloy may be attributed to the adsorption of protectors on the surface, which limits the dissolution of the magnesium alloy by way of blockading of its corrosion sites and subsequently manage the corrosion fee from 25.85 to zero.73mmy-1.

Table 4. Weight loss value of various concentrations of *4CTMBB* in 3%NaCl solution

Conc. of *4CTMBB* (ppm)	**Weight loss (mg)**	**Corrosion rate (mmy^{-1})**	**Protection Efficiency (%)**
Blank	10.5	25.85	-

10	0.7	1.72	93.34
50	0.6	1.47	94.31
100	0.6	1.47	94.31
150	0.5	1.23	95.24
200	0.4	0.98	96.20
250	0.3	0.73	97.17

3.2 *Potentiodynamic polarization study*

The parameters acquired from electrochemical measurements consisting of corrosion capability (Ecorr), corrosion modern-day (Icorr), anodic and cathodic Tafel slopes (βa and βc) and safety efficiency PE% are given in desk five.The Ecorr values do now not trade in a regular manner from the clean value. This shows that the protector works via combined kind of protection. it's far obvious from discern five, that Tafel curves are shifted markedly to lower corrosion modern-day density in the presence of protector (250ppm 4CTMBB). The Icorr value lower from the blank price (2.897 to 0.168A/cm2×10-five), this decrease in Icorr is a protection of elevated protection efficiency (ninety four). The βa and βc slopes values equally shifted inside the addition of protector from the clean, this means that the 4CTMBB acts as a combined kind protector. In other words, both anodic and cathodic reactions of magnesium alloy electrode are notably blanketed via 4CTMBB compound .

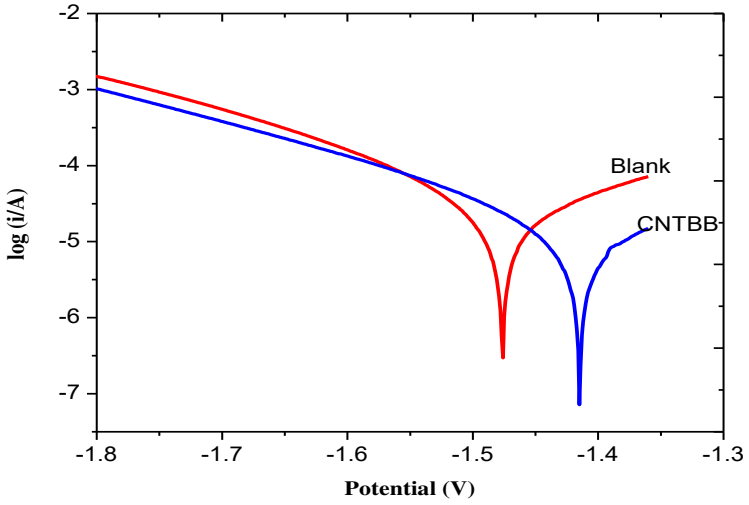

Figure 5. Tafel polarization plots of magnesium alloy (a) 3% NaCl solution (blank) (b) 3% NaCl solution with 250ppm 4CTMBB

Table 5. Tafel parameters for the corrosion of magnesium in 3% NaCl in the absence and presence of protector obtained from potentiodynamic polarization technique

Concentration of 4CTMBB (ppm)	Tafel parameters				PE_p (%)
	E_{corr} mV vs SCE	I_{cor-r} A/cm^2×10^{-5}	β_a mV/decade	β_c mV/decade	
Blank	-147.6	2.897	180.1	134.5	-
250	- 139.8	0.168	595.9	145.0	94.4

3.4 Impedance Spectra

The impedance method presents facts approximately the corrosion safety manner. Nyquist plots of magnesium alloy in 3% NaCl solution in the absence and presence of protector are proven in figure 6.The impedance spectra show off a unmarried semicircle for a particular concentration and the diameter of semicircle boom inside the presence of protector. The Nyquist plots do no longer gift best semi-circle, they display a depressed capacitive loop within the high frequency range. these deviation from ideal round form, regularly referred to as frequency dispersion became attributed to surface roughness and in homogeneities of the strong surface. moreover, the impedance reaction of magnesium alloy with 3% NaCl by myself has changed notably after addition of the protector. The most effective becoming is represented by Rundles electric equivalent circuits used to healthy the experimental outcomes have been as previously pronounced . The interfacial double layer capacitance (Cdl) values had been estimated from the impedance price using Nyquist plot with the aid of the system.

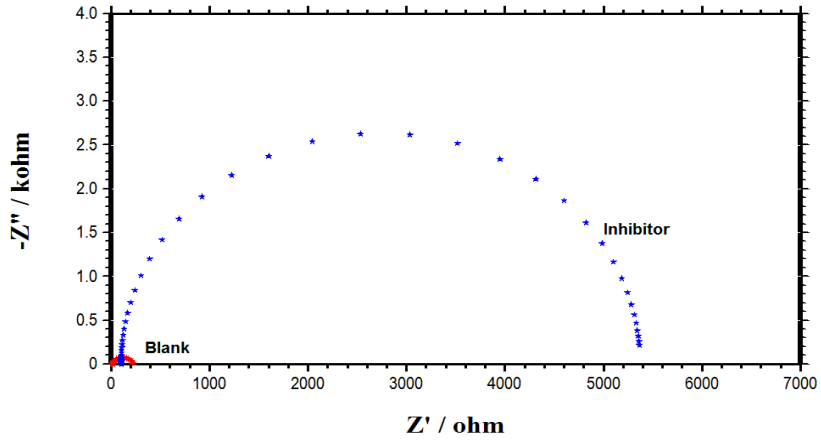

Figure 6: Nyquist plots of magnesium alloy in the absence and presence of 4CTMBB

$$f(-Zmax'') = \frac{1}{2\pi C_{dl} R_{ct}}$$

This decrease in Cdl fee additionally suggests the sluggish substitute of chloride and water molecule by using the adsorption of the protector at the steel surface, reducing value of steel dissolution [5]. The boom in Rct from 213.1 to 5268.6 Ωcm2 values in the presence of protector is because of the formation of defensive film at the metal/solution interface. The table four.4.1 confirms that the PE% inside the presence of protector method has 96% PE. those observations endorse that the resistance closer to rate transfer reactions is responsible for corrosion procedure. The results as obtained by means of electrochemical research are constant with the results of the weight reduction measurements and potentiodynamic polarization observe.

Table 6. Nyquist parameters of magnesium alloy in 3% NaCl solution in the absence and presence of *4CTMBB*

Conc. of *4CTMBB* (ppm)	**R_{ct}ohm cm^2**	**C_{dl} F.cm^{-2}×10^{-6}**	**% PE_{im}**
Blank	213.1	9.558	-
250	5268.6	0.011	96

4. Scanning Electron Microscope (SEM)

Scanning electron microscopy (SEM) was analyzed to have a look at the surface morphology of the magnesium alloy immersed in one-of-a-kind solutions. Figures7a, 7b and 7c display SEM pics of polished magnesium alloy, and magnesium alloy floor in the absence and the presence of the protector method respectively. it is able to be visible from figure 7 b (10μm), that the floor is strongly damaged, fault the metallic houses and there's formation of different varieties of corrosion products (magnesium oxides) on the surface in the absence of the protector. It further suggests that the corrosion merchandise appear very choppy and the floor layer is too hard. figure 7 a (10μm) screen the good surface properties and absence of corrosion product. figure 7 a(10μm) reveal that SEM pics of polished magnesium alloy immersed within the protector solutions are in proper conditions having clean surfaces.

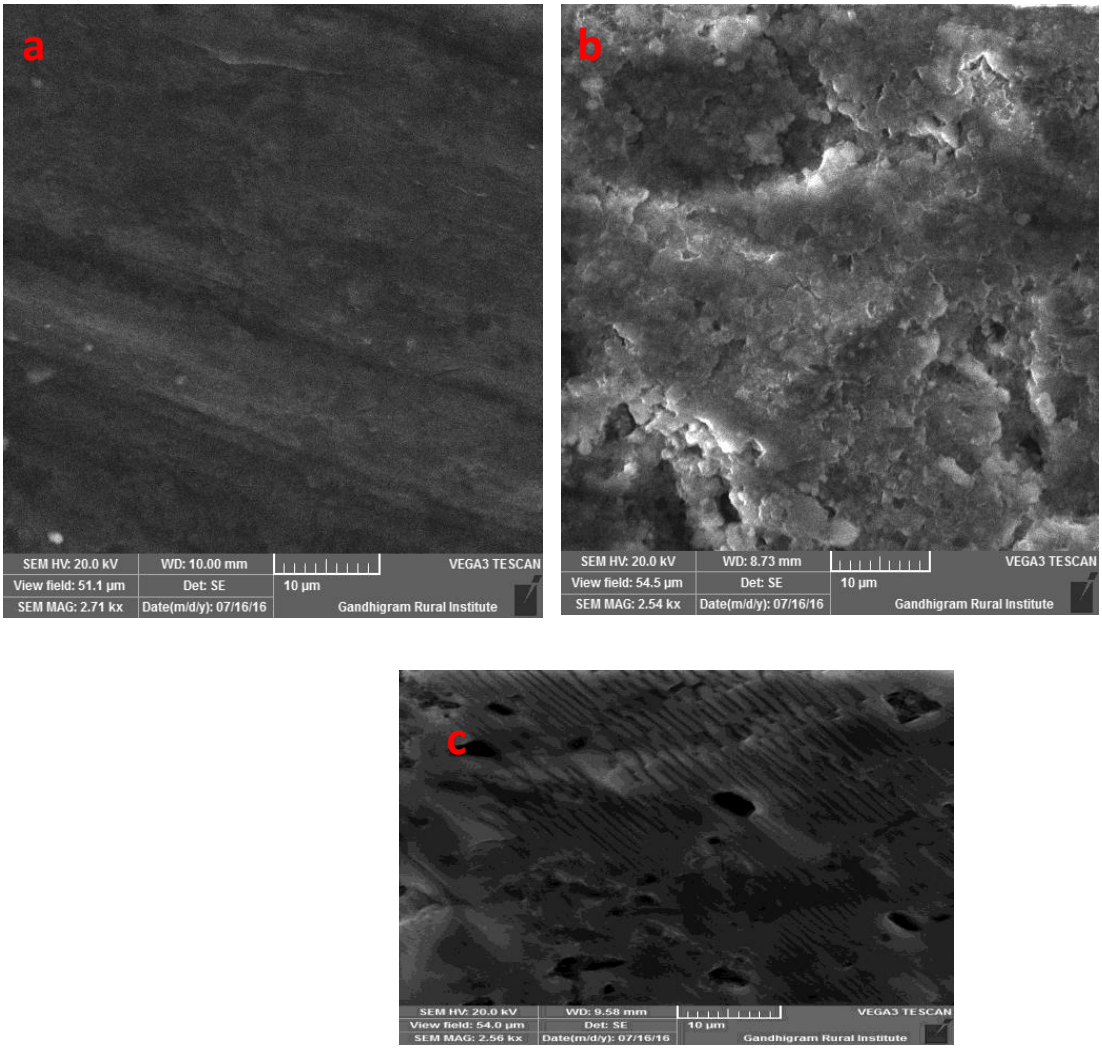

Figure4.5.1. SEM images of a) Polished magnesium alloy surface b) Blank c) Presence of protector molecule (4CTMBB) it's miles important to strain that once the protector is present in the solution, the morphology of the magnesium alloy surface are pretty specific from the previous one. it is referred to that the formation of a defensive film, that is uniformly distributed on the whole surface of the steel. this can be interpreted as due to the adsorption of the protector on the steel surface incorporating into the passive film as a way to block the active web site gift on the magnesium alloy surface. accordingly, the protective movie covers the whole metallic floor. This statement additionally money owed for the excessive safety efficiency values obtained at some stage in the 391f28ade68635a26d417ea25e9ae9c1 research of the protector device. This indicated that the protector molecules hindered the dissolution of magnesium alloy through forming a protecting movie on the magnesium alloy surface and thereby reduced the corrosion price. So, SEM evaluation shows the protecting nature of the floor film .

5. Energy Dispersive X-ray Analysis (EDX)

The composition of protective movie fashioned at the magnesium alloy floor become analyzed using EDX as proven in Fig. 8(a-c). The EDX spectrum of polished magnesium alloy pattern in Fig.8a suggests a harmony of floor composition houses, at the same time as the spectrum in case of magnesium alloy pattern immersed in absence of protector molecules was failed due to the fact it's miles significantly weakened because of the corrosion as proven in Fig.8b. Fig 8c suggests the spectrum of the presence of protector molecule. The lower of magnesium top and look of carbon, nitrogen and oxygen height turned into located because of the formation of a robust shielding movie of the protector molecules on the floor of magnesium alloy sample . The action of protector is related to adsorption and formation of a barrier film on the electrode floor. The formation of such a barrier film is confirmed through SEM and EDX examination of magnesium alloy floor.

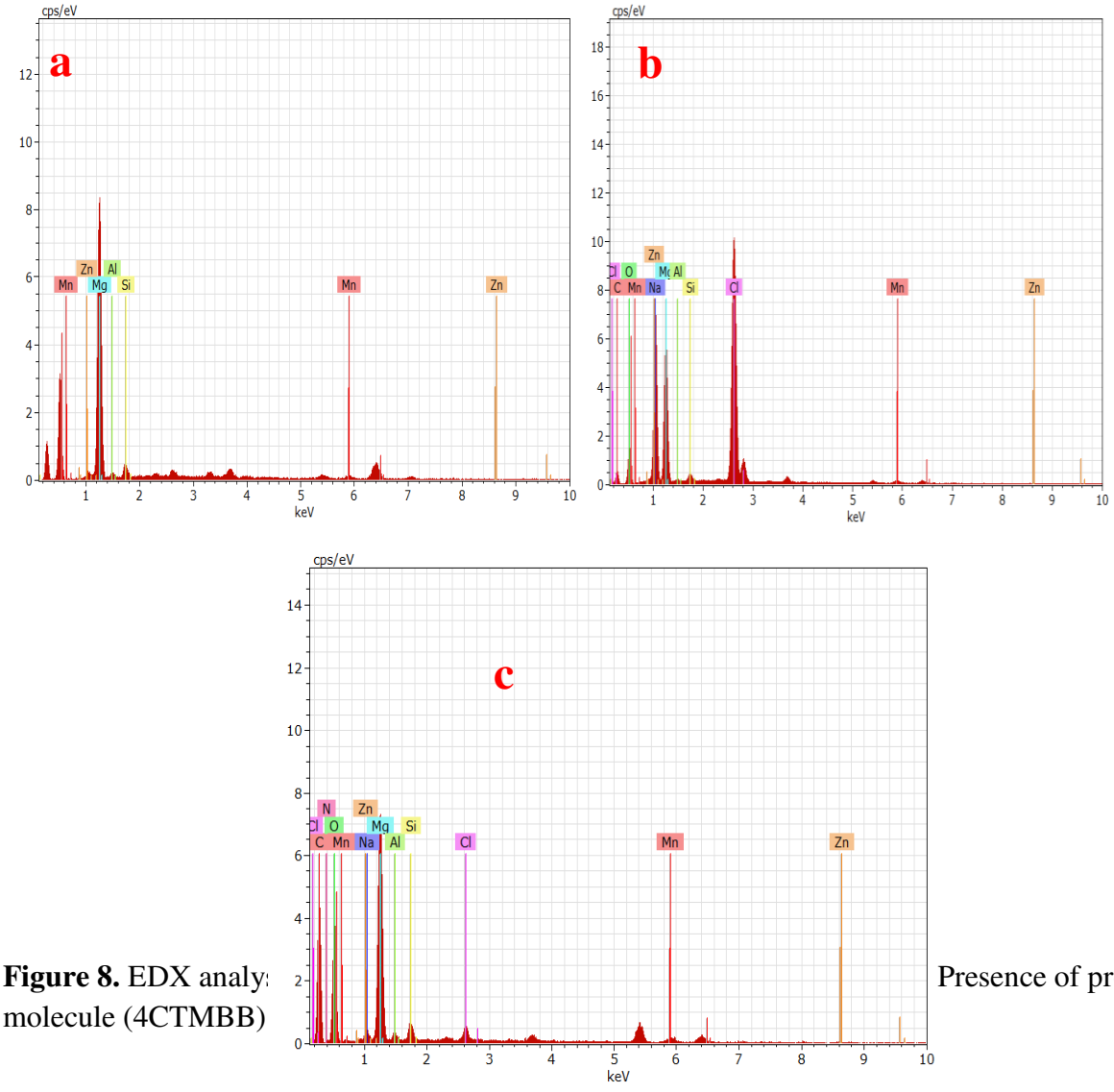

Figure 8. EDX analy Presence of protector molecule (4CTMBB)

Summary

The present study deals with the corrosion safety of magnesium alloy by means of four-Chloro-N'-(3,four,five-trimethoxybenzilidene) benzohydrazide (4CTMBB) changed into synthesized and 3% NaCl answer became prepared. The compound became showed by means of toes-IR,1H NMR,13C NMR spectra analyzed. when 4CTMBB is used as protector, it has a maximum of ninety seven% PE for 168h duration in 250ppm awareness. result acquired from weight loss, potentiodynamic polarization and AC impedance in reasonably top settlement. Polarization studies display that 4CTMBB acts as a blended sort of protector. SEM, EDX and Impedance research verify the formation of adsorption layer to protector at the magnesium alloy floor.

References

1. J.H. Nordlien, K. Nisancioglu, S. Ono, N. Masuko, J. Electrochem. Soc. 144, 461– 466.
(1997)
2. G. Baril, N. Pebere, Corros. Sci. 43, 471–484 (2001) .
3. 1. Xianghong Li, Shuduan Deng and Hui Fu, Corrosion Science, 53, 3241-3247 (2011) .
4. Singh A.K., Quraishi M. A., Corrosion Science, 53 (2011) 1288-1297.
5. B.V. AppaRao, M. VenkateswaraRao, S. SrinivasaRao, B. Sreedhar, J. Chem. Sci, 122, (2010), 639.
6. M.A.Amin, J.Appl. Electrochem.36, 215. (2006),
7. J.P. Perdew, K. Burke, M. Ernzerhof, Generalized gradient approximation made simple, Phys. Rev. Lett. 77 , 3865-3868. (1996)
8. R. Elmer, M. Berg, L. Carl en, B. Jakobsson, B. Nor en, A. Oskarsson, G. Ericsson, J. Julien, T.F. Thorsteinsen, M. Guttormsen, G. Løvhøiden, V. Bellini, E. Grosse, C. Müntz, P. Senger, L. Westerberg, Kþ emission in symmetric heavy ion reactions at subthreshold energies, Phys. Rev. Lett. 77, 4884-4886 (1996).
9. S. Grimme, Semiempirical GGA-type density functional constructed with a long-range dispersion correction, J. Comput. Chem. 27, 1787-1799. (2006)
10. G. Kresse, J. Furthmüller, Efficiency of ab-initio total energy calculations for metals and semiconductors using a plane-wave basis set, Comput. Mater. Sci. 6,) 15-50. (1996)
11. G. Kresse, J. Furthmüller, Efficient iterative schemes for ab initio total-energy calculations using a plane-wave basis set, Phys. Rev. B 54 , 11169-11186 (1996).
12. G. Kresse, J. Hafner, Ab initio molecular-dynamics simulation of the liquidmetal-amorphous-semiconductor transition in germanium, Phys. Rev. B 49, 14251-14269. (1994) .
13. G. Kresse, J. Hafner, Ab initio molecular dynamics for liquid metals, Phys. Rev. B 47 (1993) 558e561. [17] J. Bartley, N. Huynh, S.E. Bottle, H. Flitt, T. Notoya, D.P. Schweinsberg, Computer simulation of the corrosion inhibition of copper in acidic solution by alkyl esters of 5-carboxybenzotriazole, Corros. Sci. 45, 81-96. (2003).
14. Materials Studio, Accelrys Software, Inc, San Diego, CA, 2010.
15. S. Yesudass, L.O. Olasunkanmi, I. Bahadur, M.M. Kabanda, I.B. Obot, E.E. Ebenso, Experimental and theoretical studies on some selected ionic liquids with different cations/anions as corrosion inhibitors for mild steel in acidic medium, J. Taiwan Inst. Chem. E. 64, 252-268.
(2016)
16. F. Mansfeld, Recording and analysis of AC impedance data for corrosion studies, Corros. Sci. 36 , 301-307. (1981)
17. C.H. Hsu, F. Mansfeld, Technical note: concerning the conversion of the constant phase element parameter Y0 into a capacitance, Corros. Sci. 57 , 747-748. (2001)
18. Q. Qu, S. Jiang, W. Bai, L. Li, Effect of ethylenediamine tetraacetic acid disodium on the corrosion of cold rolled steel in the presence of benzotriazole in hydrochloric acid, Electrochim. Acta 52 , 6811-6820. (2007)

19. H.H. Hassan, Inhibition of mild steel corrosion in hydrochloric acid solution by triazole derivatives: Part II: time and temperature effects and thermodynamic treatments, Electrochim. Acta 53 , 1722-1730 (2007)
20 J. Zhao, G. Chen, The synergistic inhibition effect of oleic-based imidazoline and sodium benzoate on mild steel corrosion in a CO2-saturated brine solution, Electrochim. Acta 69 , 247-255 (2012)
21. F.W. Schapink, M. Oudeman, K.W. Leu, J.N. Helle, The adsorption of thiourea at a mercury-electrolyte interface, Trans. Faraday Soc. 56. 415-423 (1960) .
22. A.A. El-Awady, B.A. Abd-El-Nabey, S.G. Aziz, Kinetic-thermodynamic and adsorption isotherms analyses for the inhibition of the acid corrosion of steel by cyclic and open-chain amines, J. Electrochem. Soc. 139, 2149-2154 (1992).
23. O. Ikeda, H. Jimbo, H. Tamura, Adsorption of tetramethylthiourea at the mercury/water interface, J. Electroanal. Chem. 137, 127-141 (1982) .
24. E. Khamis, F. Bellucci, R.M. Latanision, E.S.H. El-Ashry, Acid corrosion inhibition of nickel by 2-(triphenosphoranylidene) succinic anhydride, Corrosion 47, 677-686 (1991).
25. H.P. Dhar, B.E. Conway, K.M. Joshi, On the form of adsorption isotherms for substitutional adsorption of molecules of different sizes, Electrochim. Acta 18, 789-798 (1973).
26. A. Zarrouk, B. Hammouti, A. Dafali, F. Bentiss, Inhibitive properties and adsorption of purpald as a corrosion inhibitor for copper in nitric acid medium, Ind. Eng. Chem. Res. 52, 2560-2568 (2013)
27. R.C. Zeng, Y. Hu, S.K. Guan, H.Z. Cui, E.H. Han, Corrosion of magnesium alloy AZ31: the influence of bicarbonate, sulphate, hydrogen phosphate and dihydrogen phosphate ions in saline solution, Corros. Sci. 86, 171-182 (2014).

Figures

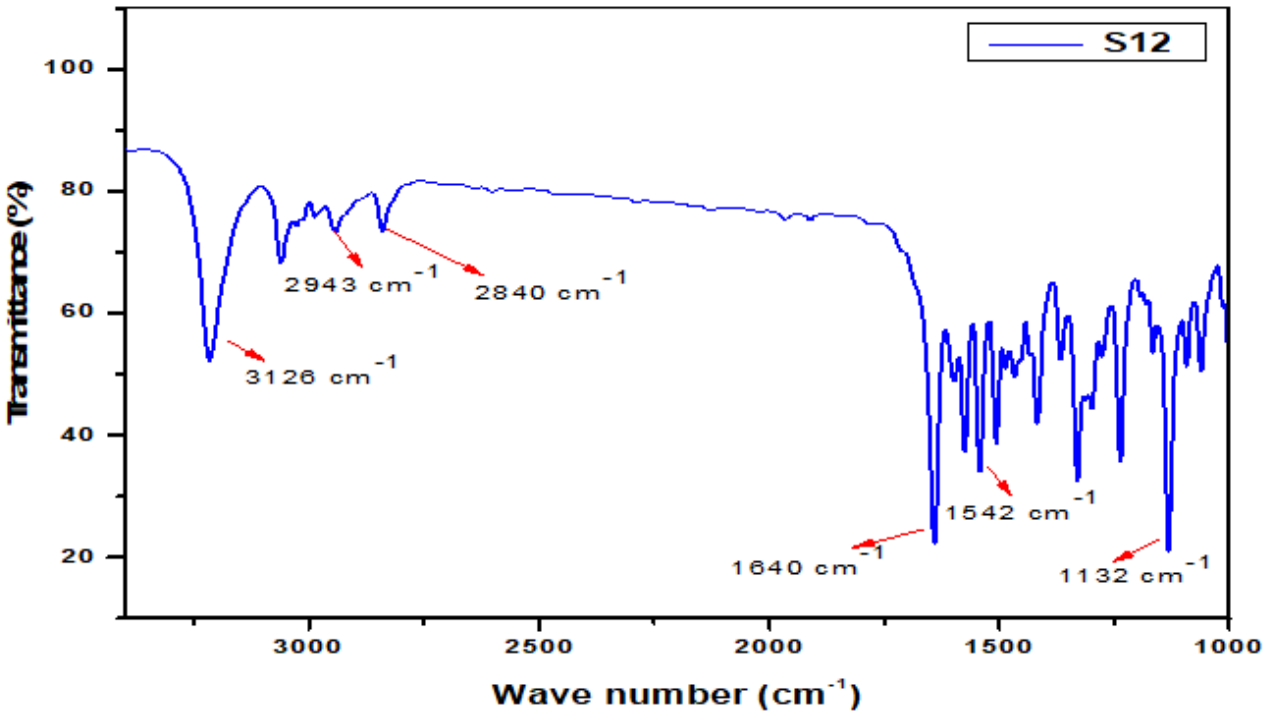

Figure 1

FT-IR spectrum of 4CTMBB

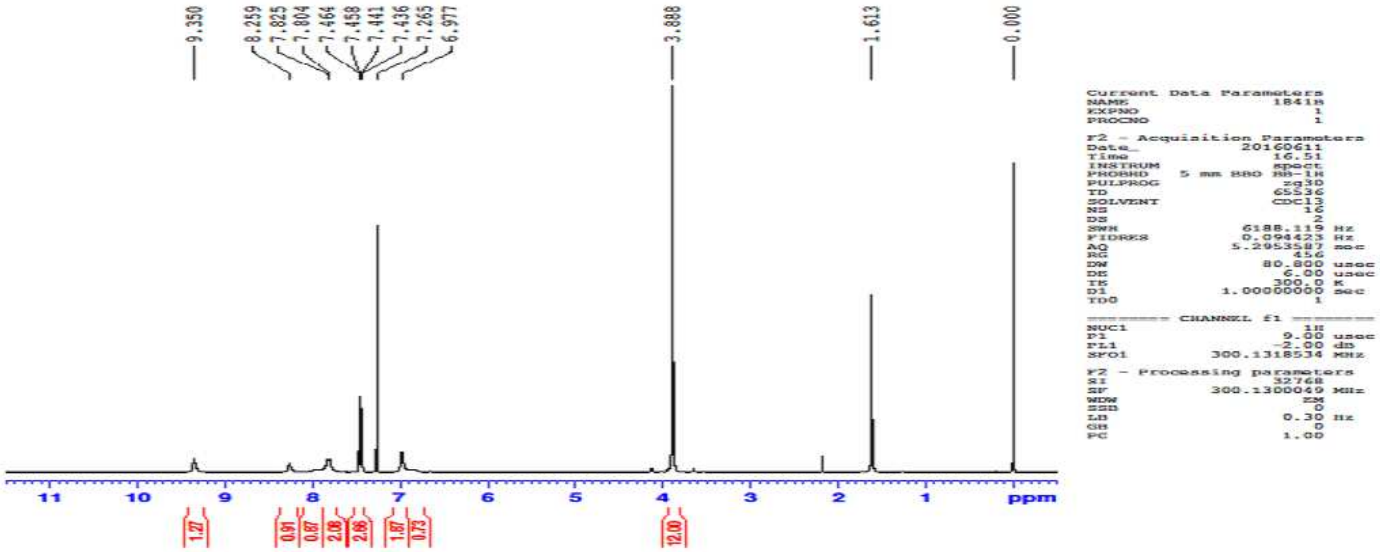

Figure 2

1H NMR spectrum of 4CTMBB

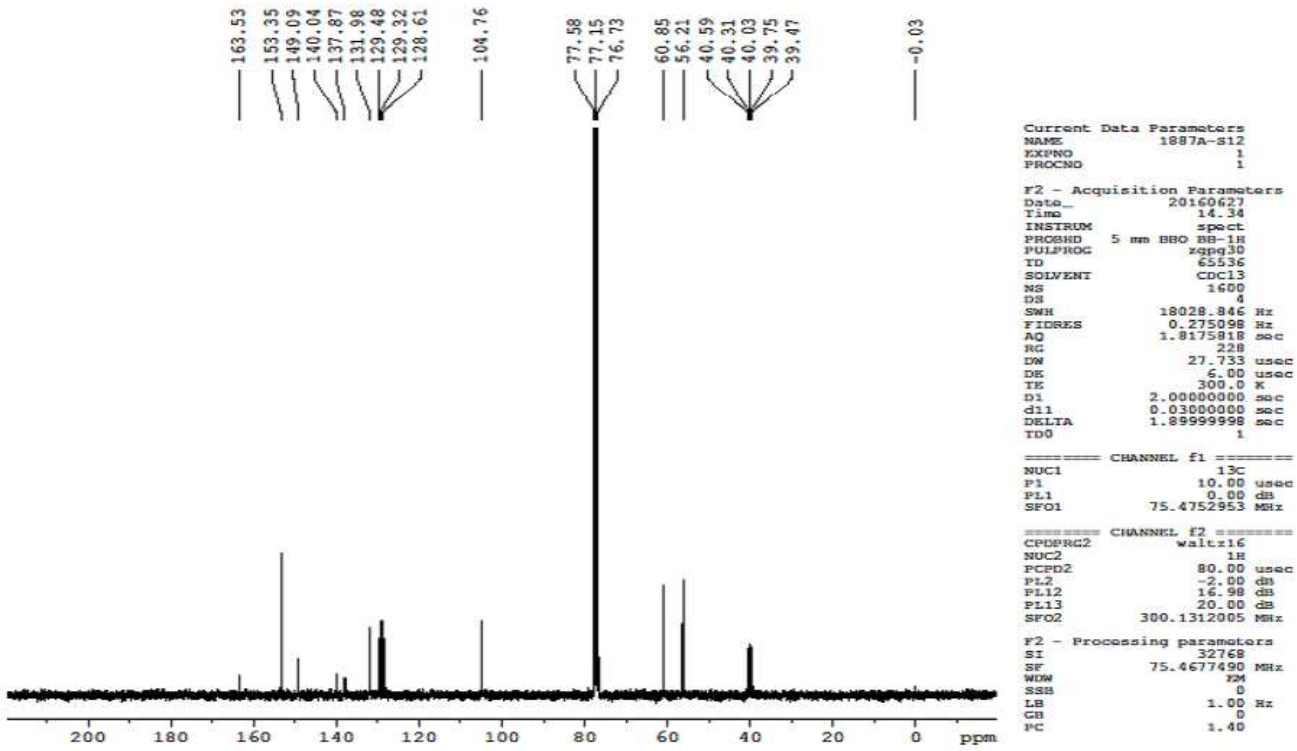

Figure 3

13C NMR spectrum of 4CTMBB

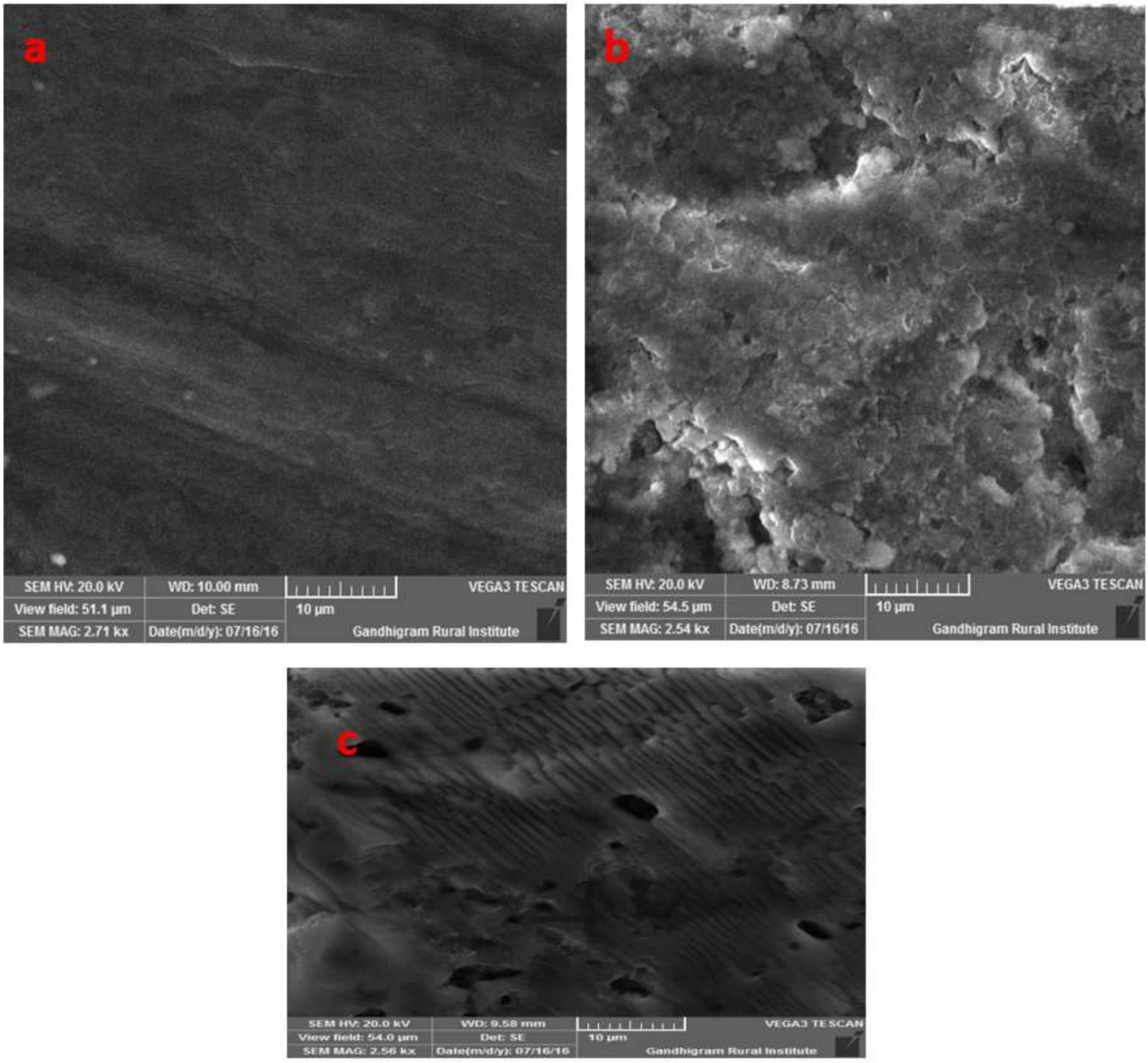

Figure 4

SEM images of a) Polished magnesium alloy surface b) Blank c) Presence of protector molecule (4CTMBB) it's miles important to strain that once the protector is present in the solution, the morphology of the magnesium alloy surface are pretty specific from the previous one. it is re-ferred to that the formation of a defensive film, that is uniformly distributed on the whole sur-face of the steel. this can be interpreted as due to the adsorption of the protector on the steel sur-face incorporating into the passive film as a way to block the active web site gift on the magnesi-um alloy surface. accordingly, the protective movie covers the whole metallic floor. This state-ment additionally money owed for the excessive safety efficiency values obtained at some stage in the 391f28ade68635a26d417ea25e9ae9c1 research of the protector device. This indicated that the protector molecules hindered the dissolution of magnesium alloy

through forming a protect-ing movie on the magnesium alloy surface and thereby reduced the corrosion price. So, SEM evaluation shows the protecting nature of the floor film .

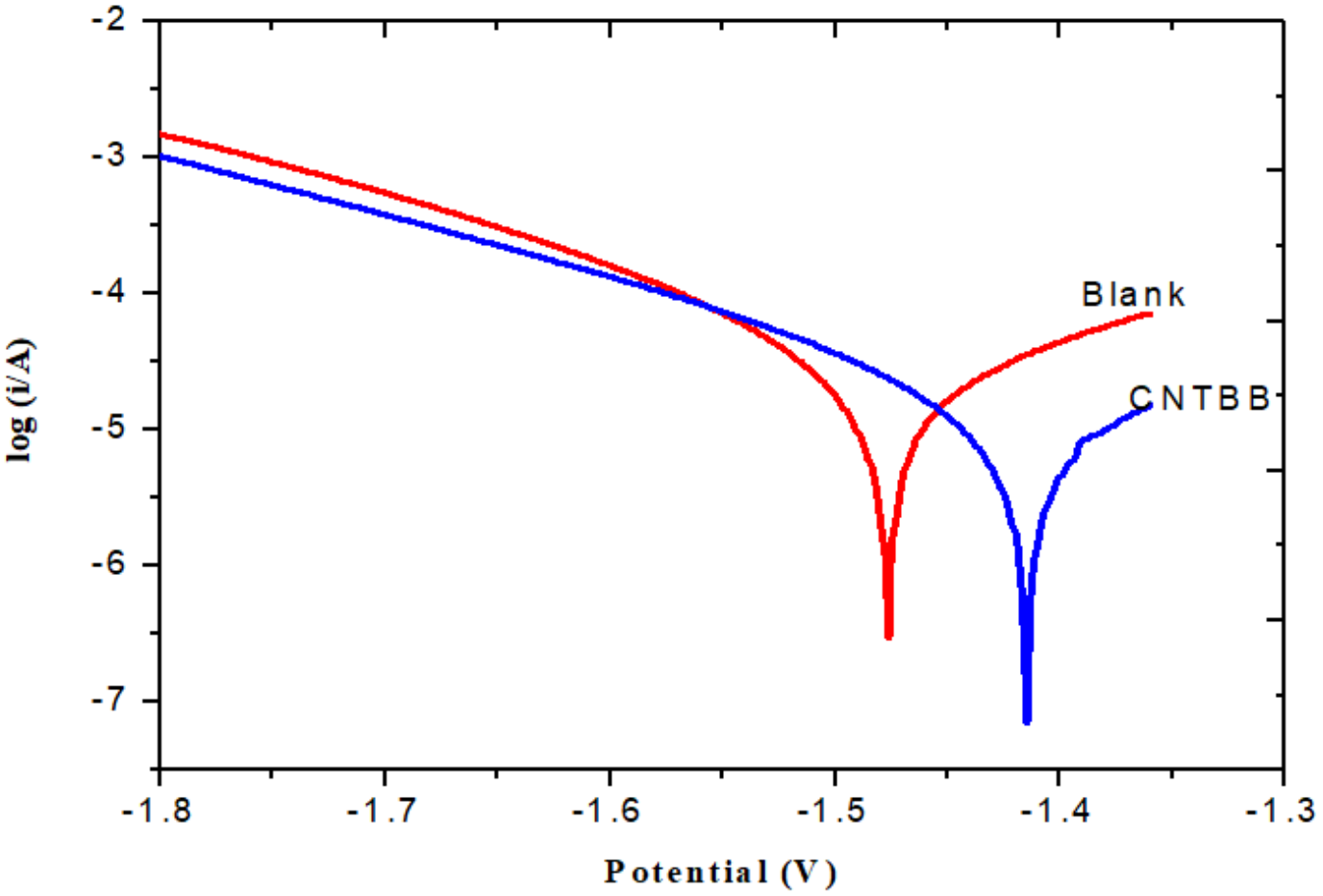

Figure 5

Tafel polarization plots of magnesium alloy (a) 3% NaCl solution (blank) (b) 3% NaCl solution with 250ppm 4CTMBB

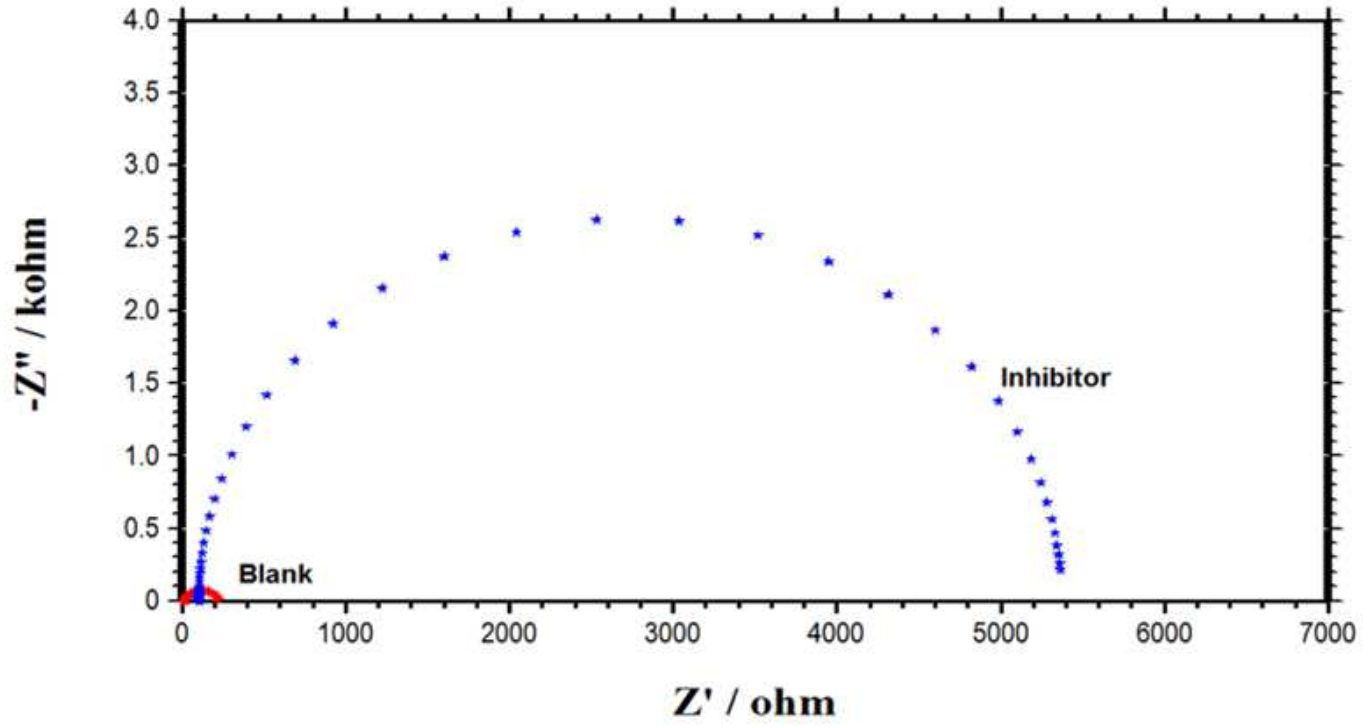

Figure 6

Nyquist plots of magnesium alloy in the absence and presence of 4CTMBB

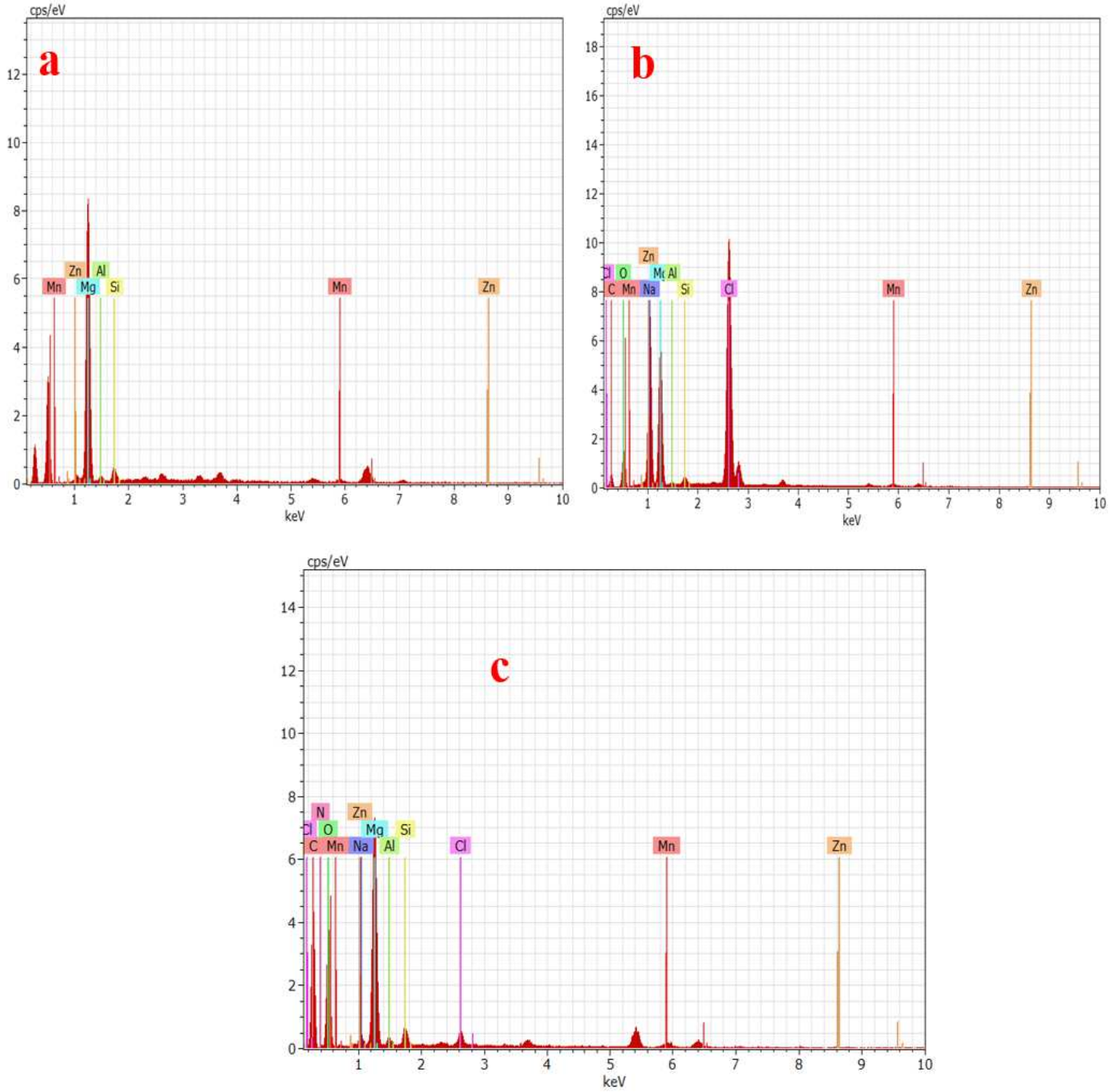

Figure 7

EDX analysis of a) Polished magnesium alloy surface b) Blankc) Presence of protector molecule (4CTMBB)

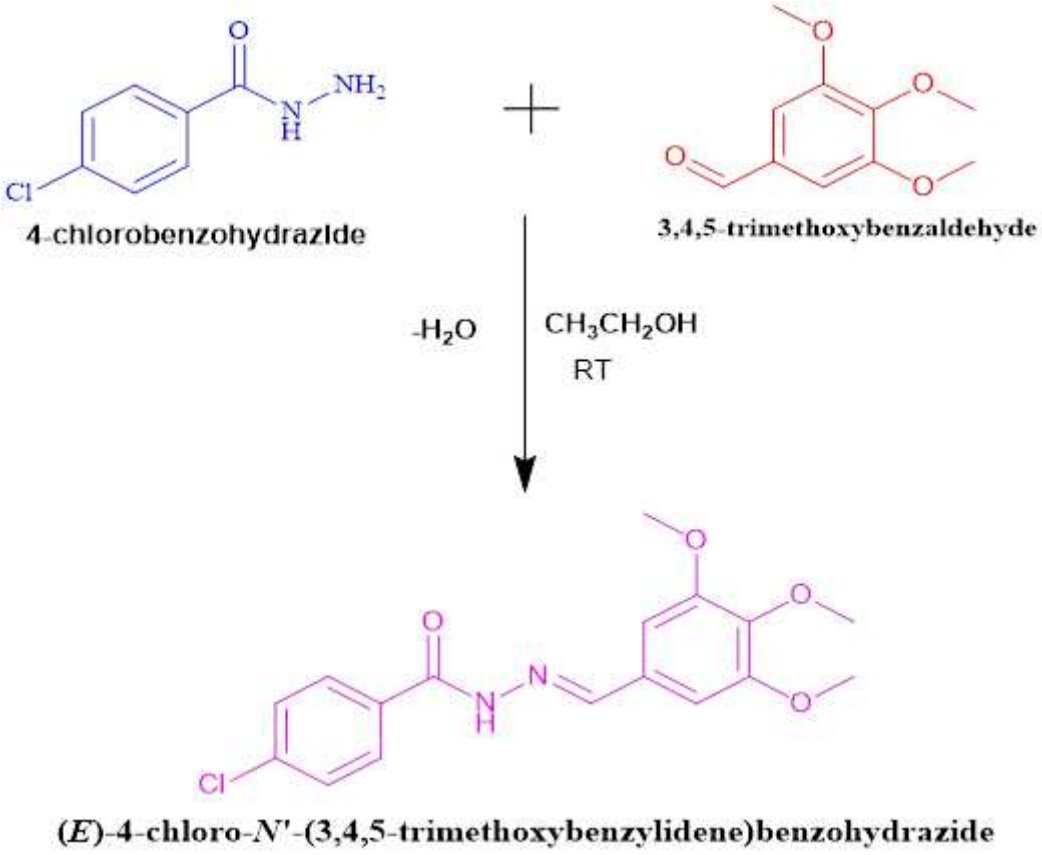

Figure 8

SCHEME